Effect of Focused Ion Beam Irradiation on Superconducting Nanowires

Lior Shani[1,2] · Avital Fried[1,2] · Yafit Fleger[2] · Olga Girshevitz[2] · Amos Sharoni[1,2] · Yosef Yeshurun[1,2]

Abstract

Recent advances in focused ion beam (FIB) technology exploit accelerated helium or neon ions, rather than gallium, for maskless fabrication of superconducting nanocomponents. We present a study of the effect of the damage induced by the accelerated ions on the superconducting transition temperature, T_c, of a patterned ~85-nm-wide Nb wire, demonstrating a decrease of T_c from ~5.5 K in the wire patterned by He ions to ~2.8 and 2.3 K exploiting Ne and Ga ions, respectively. In an effort to gain insight into the origin of these changes in T_c, we performed Stopping and Range of Ions in Matter (SRIM) simulations to estimate the damage induced by each type of ion. The simulations show that the lateral distribution of the ion beam and the sputtering rate in using Ne or Ga are significantly larger than those caused by He, consistent with the changes in the measured electrical properties of the nanowire.

1 Introduction

Improving fabrication methods has been an ongoing quest in the field of nanoscale superconducting electronics. A common technique used to fabricate sub-micron superconducting components is e-beam lithography by creating a mask in the resist and depositing superconducting material, or by applying high currents in the e-beam writer to form "crosslinked" resist followed by RIE to remove the unprotected areas [1]. Nanoscale superconducting architectures such as Superconducting Single-Photon Detectors (SNSPD) [2], nano-SQUIDs [3], and superconducting qubits [4] have been produced using this technique which, however, requires meticulous calibration, especially in ultra-narrow superconducting nanowires. Another fabrication technique exploits a bottom-up approach, coating premade structures such as carbon nanotubes [5], DNA [6], and DNA origami [7] with superconducting material. The major drawback in using such techniques is that it is very hard to make adjustments or

changes; even minor changes will often require developing a new process.

The use of a "maskless" approach based on Focused Ion Beam (FIB) has emerged as a favorable technique in producing patterns with nanometric precision. Originally, the technique used gallium (Ga), demonstrating its capabilities in obtaining selective patterning with nanometric resolution. However, the Ga Focused Ion Beam has shown a clear disadvantage in patterning superconducting nanostructures as the irradiated ions cause a degradation of the superconducting transition temperature, T_c [8, 9]. Recent developments of FIBs include the use of helium (He) and neon (Ne) ions that demonstrate the ability to produce maskless patterns with much less damages upon the superconducting nanostructures [10–12]. The major difference between Ga, Ne, and He ions is that the irradiation with Ga and Ne ions sputters the targeted area which can lead — depending on the dose — to a complete removal of the material [13], whereas He induce defects in the materials turn it into an insulator [14, 15].

Irradiation damages from He, Ne, and Ga were observed in a wide range of superconducting architectures [16–18]. Nevertheless, a comprehensive analysis of the effect of each type of irradiated ions, in general, and on the properties of the superconducting nanowire, in particular, has not yet been reported. In this work we present a study of the transport properties of ~85-nm-wide niobium (Nb) wires that were

✉ Yosef Yeshurun
  yeshurun@mail.biu.ac.il

1 Department of Physics, Bar-Ilan University,
   5290002 Ramat-Gan, Israel

2 Bar-Ilan Institute of Nanotechnology and Advanced
   Materials (BINA), 5290002 Ramat-Gan, Israel

prepared using Ga, He, and Ne ion irradiation and measure their transport properties. The results show a clear dependence of T_c on the ions used. To get insight into these results, we performed a Stopping and Range of Ions in Matter (SRIM) simulations. The simulations show that the lateral distribution of the ion beam and the sputtering rate increase significantly in using Ne or Ga instead of He, consistent with the changes in the measured electrical properties of the nanowire.

2 Sample Preparation

A 20-nm-thick film of Nb on a silicon (Si) was prepared, using magnetron sputtering (AJA International Inc.). Note that in some studies, e.g., [19], the Nb film was protected using a capping layer. In our work, we skipped this procedure as we wanted to study the direct effect of ion irradiation on the superconducting material. A pattern of 4 probes with ~ 1.5-μm-wide Nb wires connecting between large bonding pads was produced using laser lithography (MLA Heidelberg Inst.) on the Nb film, followed by removing the unprotected Nb film using BCl_3-Cl_2 RIE (Versaline ICP-RIE). The width of the wire that connects the voltage pads was then reduced from 1.5–2 μm to ~ 85 nm, using the FIB.

Figure 1a shows a SEM image of the ~ 85-nm-wide Nb wire (marked by a green arrow) that was prepared using Ga-FIB (Helios Dual-Beam, ThermoFisher) applying acceleration of 30-kV, 80-pA ion current with a dose of ~ 1.5×10^{18} ions/cm^2 and milling time of ~ 490 ms. The bright and dark areas in the image reflect the SEM contrast between the Nb film and Si substrate, respectively. The irradiated area, marked in a dashed rectangle, shows that the Nb layer was completely removed, revealing the Si substrate. Figure 1 b and c show SEM images of ~ 85-nm-wide Nb wires, marked by green arrows, that were prepared using Ne and He FIB, respectively. The applied

acceleration voltage for these wires was 30 kV, the dose was ~ 1.3×10^{18} ions/cm^2, and the currents were 0.8 and 0.3 pA for the He and Ne, respectively, and the irradiation time was ~ 20 min. The applied dose is required to destroy the conductivity of the Nb that is in the irradiated area [14], thus producing a nanowire that is confined by an insulating constriction. We note that in the case of the Ne, in this particular dose used, there was no significant amount of material removal. Figure 1c shows deformations that exceed the patterned area, the nanowire dimensions. High doses of He ions give rise to mechanical deformations (swelling) due to the accumulation of the He atoms that produce sub-surface nanobubbles that coalesce to form microbubbles [15].

3 Results and Discussion

The DC transport properties of the Nb nanowires were measured in Physical Properties Measurement System (PPMS, Quantum Design). Figure 2 shows the temperature dependence of the resistance, R (normalized to the normal resistance, R_n, at 8 K), of unirradiated Nb film (purple line) and wires prepared by Ga, Ne, and He irradiation (blue, orange, and yellow, respectively).

We calculated the resistivity, ρ, for the fabricated nanowires taking the value of the resistance before the transition, R_n. The values of the resistivity of the Ne and He nanowires and the film are $\rho_{Ne} = 7.8 \times 10^{-7}\Omega m$, $\rho_{He} = 6.375 \times 10^{-7}\Omega m$, and $\rho_{Film} = 2.06 \times 10^{-7}\Omega m$, respectively, and are comparable with bulk unirradiated Nb ($\rho_{Bulk} = 1.52 \times 10^{-7}\Omega m$). These values are lower compared to the Ga nanowire $\rho_{Ga} = 1.65 \times 10^{-6}\Omega m$ suggesting that the irradiation has inflicted damages that affected the resistivity.

The resistance temperature dependence of the film, R/R_n, shows a sharp superconducting transition at ~ 7.8 K. The wires, however, exhibit two distinct resistance drops. The first drop in all of the measured wires is attributed to the
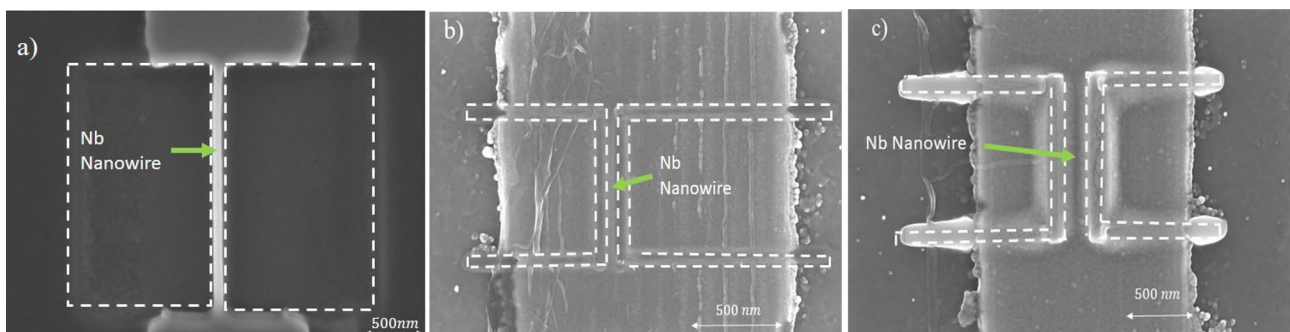

Fig. 1 HR-SEM images of Nb nanowires. **a–c** Images of the nanowires that were prepared using Ga, Ne, and He, respectively. The dashed lines enclose the irradiated areas. Note that the sputtering rate of the Nb atoms is more than 3 times larger in the case of Ga ion irradiation compared to Ne ions. Therefore, the material removal is substantially larger using Ga ions. Indeed, as clearly shown in the images, there is a total material removal for the Ga-FIB case whereas only limited material removal on the Ne-FIB case

Fig. 2 Resistance (normalized to the normal resistance, R_n, at 8 K) as a function of temperature measured at zero field. The blue, yellow, and orange lines show the temperature dependence of the nanowires that were prepared using Ga (blue), Ne (yellow), and He (orange) ions, respectively. The purple line shows the temperature dependence of an unirradiated Nb film
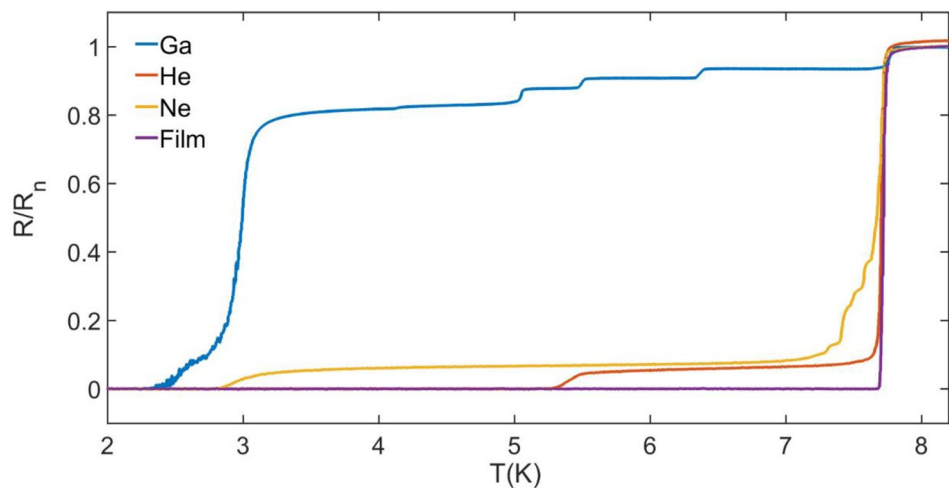
transition temperature of the film, $T_c \sim 7.8$ K. The second drop marks the transition temperature of each wire. Ga- and the Ne-irradiated wires show a transition at $T_c \sim 2.3$ K and 2.8 K, respectively, significantly lower than that measured in the He-irradiated wire, $T_c \sim 5.3$ K. The broadening of the second transition upon approaching zero resistance is ascribed to Thermally Activated Phase Slips (TAPS) that affect the resistance measured in superconducting wires with nanometric cross section [20]. Nevertheless, we note that other mechanisms such as Joule heating or inhomogeneities in the nanowires may introduce similar broadening and cannot be ruled out [21].

In order to explain the different effects of irradiation by the various ions, we performed SRIM simulations [22] that provide insights on the interaction between the ion beam at a given energy and the target atoms, i.e., the penetration depth of the energetic ions in the layer and its lateral spread along the ion beam (straggling). The central feature of SRIM is that it is based on a binary collision approach with interatomic potentials that come from quantum mechanical calculations. Panel A in Fig. 3 shows a plot of the trajectories of the various ions with atoms of the sample vs. the penetration depth of the ions. The *abscissa* represents the ion penetration depth perpendicular to the surface of the sample; the first layer is the 20-nm-thick Nb and the second layer is the Si substrate. The ordinate denotes the lateral distribution of the ions trajectories after penetration into the Nb and Si layers. Panel B in Fig. 3 shows the transverse collision distribution plot in the Nb and Si layers. The lateral distribution of He ions in the Nb layer is negligible compared to the ion distribution of the Ne and Ga in the Nb layer. Namely, most of the collisions happen in the Si. We, therefore, conclude that the wire irradiated with He ions is hardly affected by the ion bombardment. In principle, the straggling range depends strongly on the atomic number of the incident ion, and therefore, the lateral spreading of heavy ions such as Ga should

be much smaller than Ne. The SRIM simulations estimate the lateral distribution of Ne and Ga ions in a thin layer of Nb to be ~ 50 and ~ 12 nm, respectively, which implies that the Ga ions cause more damage to the Nb layer than the Ne ions. Panel C in Fig. 3 describes the projectile penetration range from the surface of the sample into its inner layers, showing 13.5 and 48.8 nm for the 30-keV Ga and Ne ions, respectively. The presence of He ions in the Nb layer is minor because the majority of the ions pass through the Nb layer and accumulate in the Si substrate. Note that the penetration depth of the Ga ions is smaller than the Nb layer thickness of 20 nm, while the 30-keV Ne ions crossover the Nb layer and are stopped in the Si substrate. In evaluating the damage inflicted upon the Nb layer, one needs to take also into account that Nb atoms at the surface of the layer may be sputtered from the sample due to recoil cascades that come back out of the target, giving surface atoms enough energy to be driven away from the target. In the case of the He as incident ion this effect is negligible (0.05 atoms/ion), while the Ne and Ga sputter 1.12 and 3.80 atoms/ion, respectively. The results imply that for Ne and Ga ions, the exposed area is extended well beyond the pre-planned borders of the pattern, penetrating into the wire and giving rise to irradiation defects.

The combined outcome of the sample sputtering and lateral distribution of the ion beam affects the electrical properties of the wire. The projectile range of the irradiated ions is affected by the atomic mass of the ions; namely, at the same acceleration energy the He ions will penetrate deeper into the surface than the Ne and Ga ions due to the relatively small mass of the He ion. The large straggle, as appears from simulations for the Ga and Ne ions, causes the high-energy ions to sputter the Nb atoms in the layer and accumulate at the edges of the nanowire, therefore affecting T_c of the irradiated nanowire. The origin of the steps that appear in the $R(T)$ curves of the nanowires irradiated by Ne and Ga (see Fig. 2)
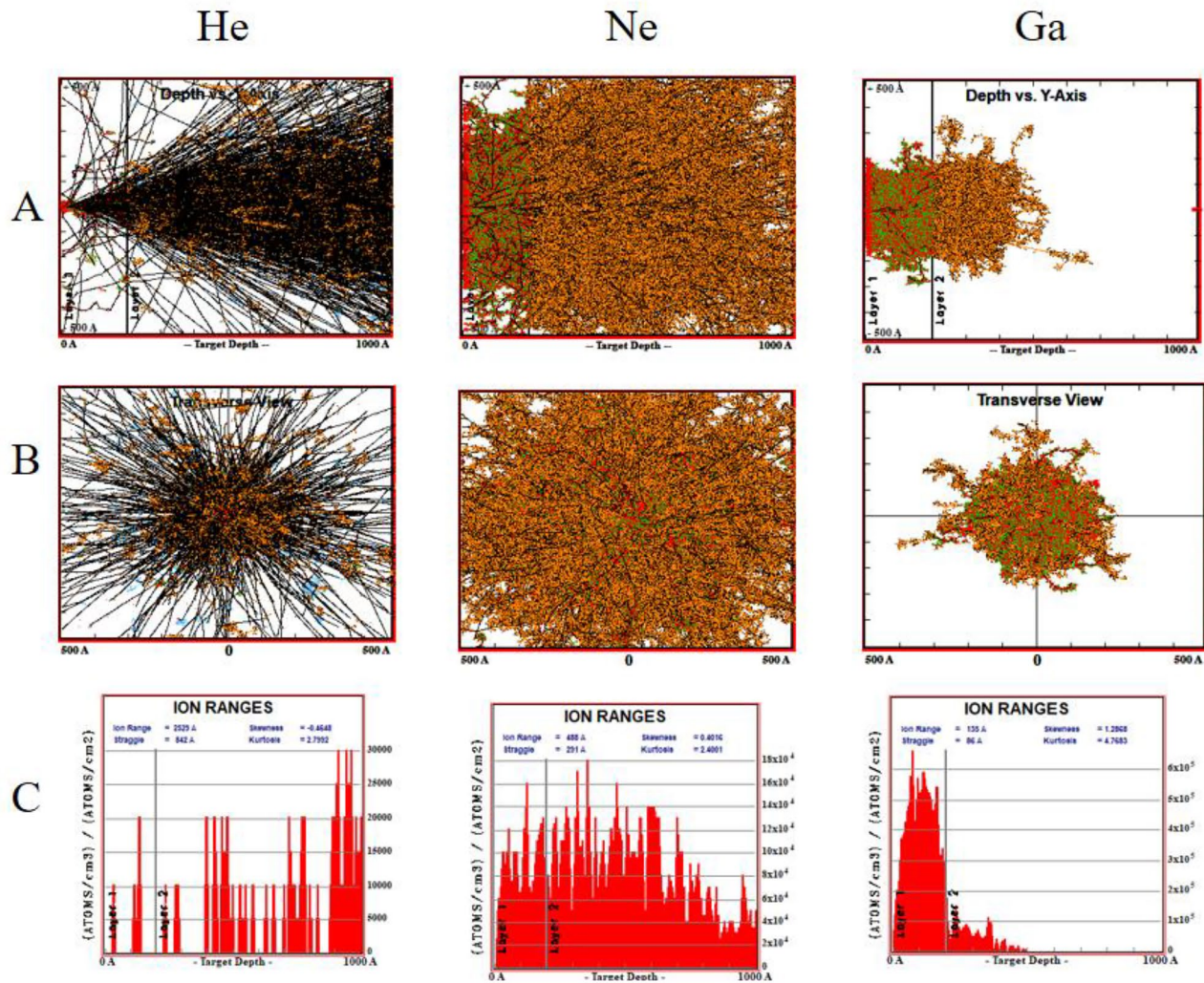
Fig. 3 **A** and **B** "Collision plots" of the irradiated ions (He, Ne, and Ga) for Nb/Si samples in lateral and transverse views, respectively. The vertical black lines in panel A denote the border between the Nb layer ("Layer 1," 20 nm thick) and the Si substrate ("Layer 2"). The trajectories of the moving ions are shown in red in the Nb layer and orange in the Si. The stopping position of the ions in the Nb and the Si are indicated by green and black, respectively. **C** The ion distribution plots perpendicular to the irradiation direction. The vertical black lines denote the border between the Nb layer (Layer 1) and the Si substrate (Layer 2). The abscissa denotes the penetration depth of the ions; the ordinate describes the concentration of the ions in units of atoms/cm^3 divided by the ion-beam dose in units of atoms/cm^2

is probably a result of a distribution of T_c in superconducting island accumulated near the edges of the wire. This explanation is somewhat supported by the simulations of panel C in Fig. 3 that show that almost all the Ga ions and a substantial amount of Ne ions accumulated in the Nb layer. In contrast, almost all of the He ions have stopped in the Si layer.

4 Conclusions

This work shows the effect of Focused Ion Beam irradiation on superconducting nanowires. Our measurements show that the irradiation damage induced by the ions affected the electrical properties of the wires, resulting in reduced T_c of

the nanowires that were prepared using Ga and Ne (~ 2.3 and 2.8 K, respectively) compared to the one that was fabricated using He (~ 5.5 K). The nanowires that were prepared using Ga and Ne ions exhibit a multi-step transition — a feature that was not observed in the nanowire prepared using He ions — probably reflecting distribution of T_c in each of these wires. The SRIM simulations show that relatively large lateral distribution of the Ga and Ne ion beams and, therefore, the exposed area is extended beyond the borders of the planned pattern. Namely, ions penetrate into the wire and sputter Nb atoms, giving rise to extended irradiation damage, thus affecting the electric properties of the wire. The results of this work demonstrate that the damage caused by FIB irradiation from different ion sources has to be taken

into account when producing maskless nanometric patterns for superconducting components.

References

1. Chen, Y.: Nanofabrication by electron beam lithography and its applications: a review. Microelectron. Eng. **135**, 57–72 (2015)
2. Holzman, I., Ivry, Y.: Superconducting nanowires for single-photon detection: progress, challenges, and opportunities. Advanced Quantum Technologies **2**, 1800058 (2019)
3. Wernsdorfer, W.: From micro-to nano-SQUIDs: applications to nanomagnetism. Superconductor Science and Technology **22**, 064013 (2009)
4. Krantz, P., Kjaergaard, M., Yan, F., Orlando, T.P., Gustavsson, S., Oliver, W.D.: A quantum engineer's guide to superconducting qubits. Applied Physics Reviews **6**, 021318 (2019)
5. Bezryadin, A., Lau, C., Tinkham, M.: Quantum suppression of superconductivity in ultrathin nanowires. Nature **404**, 971–974 (2000)
6. Hopkins, D.S., Pekker, D., Goldbart, P.M., Bezryadin, A.: Quantum interference device made by DNA templating of superconducting nanowires. Science **308**, 1762–1765 (2005)
7. Shani, L., Tinnefeld, P., Fleger, Y., Sharoni, A., Shapiro, B.Y., Shaulov, A., Gang, O., Yeshurun, Y.: DNA origami based superconducting nanowires. AIP Advances **11**, 015130 (2021)
8. Tettamanzi, G., Pakes, C., Potenza, A., Rubanov, S., Marrows, C., Prawer, S.: Superconducting transition in Nb nanowires fabricated using focused ion beam. Nanotechnology **20**, 465302 (2009)
9. Joshi-Imre, A., Bauerdick, S.: Direct-write ion beam lithography. J. Nanotechnol. 2014 (2014)
10. Shani, L., Michelson, A.N., Minevich, B., Fleger, Y., Stern, M., Shaulov, A., Yeshurun, Y., Gang, O.: DNA-assembled superconducting 3D nanoscale architectures. Nat. Commun. **11**, 1–7 (2020)
11. Burnett, J., Sagar, J., Kennedy, O.W., Warburton, P.A., Fenton, J.C.: Low-loss superconducting nanowire circuits using a neon focused ion beam. Physi. Rev. Appl. **8**, 014039 (2017)
12. Kennedy, O., Burnett, J., Fenton, J., Constantino, N., Warburton, P., Morton, J., Dupont-Ferrier, E.: Tunable Nb superconducting resonator based on a constriction nano-SQUID fabricated with a Ne focused ion beam, Phys. Rev. Appl. **11**, 014006 (2019)
13. Potter, J., Kennedy, O.W., Fenton, J.C., Warburton, P.A.: Nonlinear quantum processes in superconducting resonators terminated by neon-focused-ion-beam-fabricated superconducting nanowires. IEEE Trans. Appl. Supercond. **30**, 1–4 (2020)
14. Cybart, S.A., Cho, E., Wong, T., Wehlin, B.H., Ma, M.K., Huynh, C., Dynes, R.: Nano josephson superconducting tunnel junctions in yba 2 cu 3 o 7−δ directly patterned with a focused helium ion beam. Nat. Nanotechnol. **10**, 598–602 (2015)
15. Martinez, G.D., Buckley, D., Charaev, I., Dane, A., Dow, D.E., Berggren, K.K.: Superconducting nanowire fabrication on niobium nitride using helium Ion irradiation, arXiv preprint arXiv: 2003.02898 (2020)
16. Stritzker, B.: Superconductivity in irradiated palladium. Phys. Rev. Lett. **42**, 1769 (1979)
17. Porrati, F., Keller, L., Gspan, C., Plank, H., Huth, M.: Electrical transport properties of Ga irradiated W-based granular nanostructures. J. Phys. D Appl. Phys. **50**, 215301 (2017)
18. Moll, P.J.: Focused ion beam microstructuring of quantum matter. Annual Review of Condensed Matter Physics **9**, 147–162 (2018)
19. Lam, S.K., Bendavid, A., Du, J.: Hot spot formation in focused-ion-beam-fabricated YBa2Cu3O7− x nanobridges with high critical current densities. Nanotechnology **30**, 325301 (2019)
20. Arutyunov, K.Y., Golubev, D.S., Zaikin, A.D.: Superconductivity in one dimension. Phys. Rep. **464**, 1–70 (2008)
21. Annunziata, A.J., Quaranta, O., Santavicca, D.F., Casaburi, A., Frunzio, L., Ejrnaes, M., Rooks, M.J., Cristiano, R., Pagano, S., Frydman, A.: Reset dynamics and latching in niobium superconducting nanowire single-photon detectors, J. Appl. Phys. **108**, 084507 (2010)
22. Stoller, R.E., Toloczko, M.B., Was, G.S., Certain, A.G., Dwaraknath, S., Garner, F.A.: On the use of SRIM for computing radiation damage exposure. Nucl. Instrum. Methods Phys. Res., Sect. B **310**, 75–80 (2013)